VERSITA

Central European Journal of **Physics**

New method and treatment technique applied to interband transition in GaAs$_{1-x}$P$_x$ ternary alloys

Cristina-Mihaela Băleanu[1], Raoul R. Nigmatullin[2], Saime Sebnem Cetin[3], Dumitru Băleanu[4]*, Suleyman Ozcelik[3]†

1 University of Bucharest, Faculty of Physics, Magurele-Bucharest, Romania and National Mihail Sadoveanu High School, District 2, Bucharest, Romania

2 Theoretical Physics Department, Kazan State University, Kazan 420008, Tataristan, Russia

3 Gazi University, Faculty of Art and Sciences, Department of Physics, Teknikokullar, Ankara 06500, Turkey

4 Çankaya University, Faculty of Art and Sciences, Department of Mathematics and Computer Sciences, Ankara 06530, Turkey

Abstract: In this paper we presented a new method (Eigen-Coordinates (ECs)) that can be used for calculations of the critical points (CPs) energy of the interband-transition edges of the heterostructures. This new method is more accurate and complete in comparison with conventional ones and has a wide range of application for the calculation of the fitting parameters related to nontrivial functions that initially have nonlinear fitting parameters that are difficult to evaluate. The new method was applied to determine the CPs energies from the dielectric functions of the MBE grown GaAs$_{1-x}$P$_x$ ternary alloys obtained using spectroscopic ellipsometry (SE) measurements at room temperature in the 0.5-5 eV photon energy region. The obtained results are in good agreement with the results of the other methods.

PACS (2008): 07.60.Fs, 81.15.Hi, 78.66.Fd, 73.61.Jc, 71.20.Nr

Keywords: Eigen-coordinates method • critical points energy • spectroscopic ellipsometry • MBE • GaAsP
        © Versita Sp. z o.o.

1.   Introduction

In the semiconductor heterostructures, the energy band E_1, E'_0 and E_2 occur at the Λ, Γ and X valleys near the Brillouin zone boundary. The energy bands in the higher levels above E_0, which occur at Γ points, are split due to spin–orbit interactions. Determining the energy band structure variations on alloy composition in heterostructures is important in the design of opto–electronic devices. The composition dependence of the higher energy gaps (named critical energy points) and spin–orbit splitting energy can be obtained by evaluation of the dielectric function (DF). The DFs and optical properties of the semiconductor structures can be obtained precisely by evaluation of spectroscopic ellipsometry (SE) measurements [1–5]. To determine the CP energies from DF for a layer or layered semiconductor structures several models were developed through Harmonic Oscillator Approximation (HOA)

*E–mail: dumitru@cankaya.edu.tr
†E–mail: sozcelik@gazi.edu.tr (Corresponding author)

and Effective–Medium Approximation (EMA), which are reviewed in Ref. [6]. For analyzing the suitable CP energies for thick epitaxial layers, Yoon et al. suggested that the associated optical properties of the grown layer can be considered as the characteristics of bulk material, if the layer thickness is over the critical thickness [7].

In our previous works, the CP energies of the GaAs$_{1-x}$P$_x$/GaAs (100) ternary alloys were obtained by line–shape analysis on their dielectric functions. Alloy compositions of the alloys were determined using high resolution X–ray diffraction [1]. Also, a bowing parameter of the band gap energy was obtained from SE study due to disordered phosphorous content. In this paper we presented a new method that can be used for calculations of the critical points energies and the bowing parameter of band gap energy due to disordered phosphorous content of GaAs$_{1-x}$P$_x$/GaAs (100) ternary alloys, which are grown by using MBE [1]. This new method enables transformation of a wide class of functions, initially containing a set of nonlinear fitting parameters, into a set of slope lines [8]. It is more accurate and complete in comparison with conventional methods and has a wide range of application for calculation of the fitting parameters related to nontrivial functions that initially have nonlinear fitting parameters that are difficult to evaluate. The detailed calculations are depicted in the Mathematical Appendix.

2. Experimental procedure

Semiconducting p–n junction GaAs$_{1-x}$P$_x$ ternary alloys (A1–A5) with different phosphorous contents on epiready n–GaAs (100) substrate were grown by using a solid source V80H–MBE system with continues growth method. The lattice–match structures were obtained by growing a 1 μm thick graded index n–GaAsP layer on n–GaAs buffer layer. The p–n junction structures were obtained by growing a thick p–GaAsP layer on a n–GaAsP layer as presented in Figure 1, schematically. The growth procedure can be seen in Ref. [1], in detail.

The dielectric functions of the structures were obtained by using the Jobin Yvon variable angle spectroscopic rotating analyzer ellipsometry, which has an energy resolution of 0.01 eV. The ellipsometric data were recorded in 0.5–5 eV photon energy region with 0.01 eV increments. The angle of incidence of the light beam was fixed at 70° on the surface of the samples. The SE measurements for the samples were made at room temperature under atmospheric conditions [1]. Before the measurements, the surface of the samples was cleaned using methanol to remove any contamination artifacts. Preceding the cleaning step, the sample was rinsed thoroughly in deionized water with a
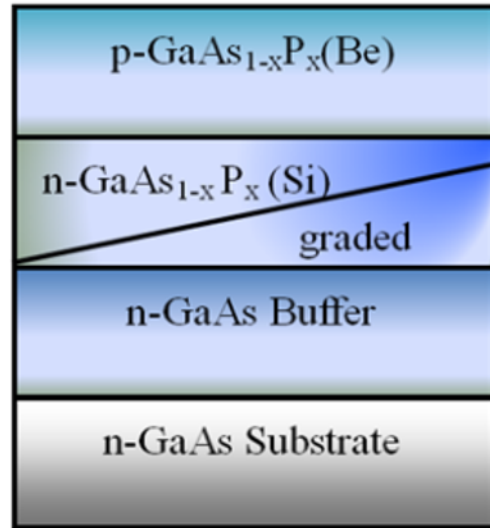

Figure 1. Schematic structure of the grown GaAs$_{1-x}$P$_x$/GaAs heterostructures [1].

resistivity of 18 MΩ–cm.

3. Application of the ECs method for calculation of the CP energies

3.1. Eigen-Coordinates (ECs) method

The main question regarding ECs method is in what cases one can obtain the basic linear relationship (BLR) for the function that initially contains a set of nonlinear fitting parameters? If this procedure can be realized for a set of functions which initially contain nonlinear fitting parameters, then the nonlinear mean–square method can be reduced to the routine procedure which is known as the linear least square method (LLSM). This reduction is important because in many cases it provides the *global* fitting minima in the space of the fitting parameters.

In order to obtain the positive answer it is necessary to obtain the corresponding differential equation that is satisfied by the chosen hypothesis. If the unknown parameters $\{C_k \ (k = 1, 2, \ldots, s)\}$ of the corresponding differential equation form a linear combination (the set of parameters can be related with initial set of parameters $\{A_l \ (l = 1, 2, \ldots, q)\}$ in a nonlinear way) then the answer for the question posed above is positive, and in other cases is negative.

The basic principles of the ECs method are outlined in

Cristina-Mihaela Băleanu, Raoul R. Nigmatullin, Saime Sebnem Cetin,
Dumitru Băleanu, Suleyman Ozcelik

[8, 9]. The application in detection of impedances and dielectric spectroscopy can be found in references [10–22]. The reader can find some information about the application in recognition of different statistical distributions in [23–25] and to dynamical chaos in [26].

It is known that the complex reflectance ratio of the polarized light

$$\rho = \frac{r_p}{r_s} = \tan(\Psi)e^{i\Delta}$$

is determined by the SE technique. Here, r_p and r_s are the reflection coefficient of the polarized light (p and s refer to parallel and perpendicular to the plane of incidence, respectively) and Ψ and Δ are ellipsometric data. The dielectric function $\varepsilon = \varepsilon_1 + \varepsilon_2$ (ε_1 and ε_2 are the real and imaginary part of the DF, respectively) of the sample was obtained by

$$\varepsilon = \sin^2 \varphi + \sin^2 \varphi \tan^2 \varphi \frac{(1-\rho)^2}{(1+\rho^2)}, \qquad (1)$$

where φ is angle of incidence of the light beam [2, 3, 27]. In this paper we used the ECs method to determine the suitable CP energies of the GaAsP ternary alloys from DF spectra, given by

$$\varepsilon(E) = C - Ae^{i\Phi}(E - E_c + i\Gamma)^n, \qquad (2)$$

where A is the amplitude, E is the photon energy, E_c is the critical point energy, Γ is the broadening factor and Φ is the excitonic phase angle. The exponent n has the values of $-\frac{1}{2}, 0, \frac{1}{2}$, and -1 for the one-dimensional, two-dimensional, three-dimensional, and excitonic critical points, respectively [1–5].

It is noted that C, A, Φ, E_c and Γ are the fitting parameters. In the case of $n \neq 0$, by applying the ECs method we obtained:

$$Y = C_1 X_1 + C_2 X_2 + C_3 X_3 + C_4 X_4 + C_5 X_5, \qquad (3)$$

where

$$\begin{aligned}
Y &= yE^2 - (n+2)\int yE\,dE - \langle \ldots \rangle, \\
X_2 &= y - \langle \ldots \rangle, \\
X_3 &= \frac{nE^2}{2} - \langle \ldots \rangle, \\
X_4 &= n\int z\,dE, \\
X_5 &= nE - \langle \ldots \rangle.
\end{aligned} \qquad (4)$$

In addition we have:

$$\begin{aligned}
C_1 &= E_c, \\
C_2 &= -\left(E_c^2 + \Gamma^2\right), \\
C_3 &= C, \\
C_4 &= \Gamma,
\end{aligned}$$

and

$$C_5 = CE_c \qquad (5)$$

such that $C_5 = C_1 \cdot C_3$ and $C_2 = -(C_1^2 + C_4^2)$, respectively. Finally, the parameters Γ and Φ have the following forms:

$$\Gamma = \left[-\left(E_c + C_2^2\right)\right]^{\frac{1}{2}}$$

and

$$\Phi = \arctan\left(\frac{-2C_2\Gamma}{C_3 + 2C_2 AE_c}\right). \qquad (6)$$

For the next case, $n = 0$, we obtained the fitting parameters C, A, Φ, E_c, Γ by applying ECs method as follows:

$$Y = C_1 X_1 + C_2 X_2 + C_3 X_3 + C_4 X_4, \qquad (7)$$

where

$$Y = yE^2 - 2\int yE\,dE - \langle \ldots \rangle \qquad (8)$$

and

$$\begin{aligned}
X_1 &= yE - \int y\,dE - \langle \ldots \rangle, & C_1 &= 2E_c, \\
X_2 &= y - \langle \ldots \rangle, & C_2 &= -\left(E_c^2 + \Gamma^2\right), \\
X_3 &= E^2 - \langle \ldots \rangle, & C_3 &= -\frac{A\cos\Phi}{2}, \\
X_4 &= E - \langle \ldots \rangle, & C_4 &= A\cos\Phi E_c - \Gamma A\sin\Phi.
\end{aligned} \qquad (9)$$

Hence, the fitting parameters E_c, Γ, A and Φ can be obtained as

$$\begin{aligned}
E_c &= \frac{C_1}{2}, \\
\Gamma &= \pm\sqrt{-C_2 - \frac{C_1^2}{4}},
\end{aligned} \qquad (10)$$

and

$$A \cos \Phi = -2C_3,$$
$$A\Gamma \sin \Phi = -C_1 C_3 - C_4,$$

and

$$A \sin \Phi = -\frac{(C_1 C_3 + C_4)}{\sqrt{-C_2 - \frac{C_1^2}{4}}}.$$

(11)

4. Results and discussions

In the present study, we suggested a new method that was used for calculations of the critical points energies and the bowing parameter of the band gap energy due to disordered phosphorous content of the MBE grown GaAs$_{1-x}$P$_x$/GaAs (100) ternary alloys. In our previous works, the CP energies and band gap bowing parameter due to the disordered phosphorous in the layers of the structures were calculated by using a second derivative method [1, 5]: The second–derivative spectra (in Figure 3 in Ref. [1]),

$$\frac{\partial^2 \varepsilon}{\partial E^2},$$

of the real parts of experimental DF were used to perform the line–shape analyses calculated numerically. The calculated second–derivative spectra were fitted to standard critical–point line shapes. The obtained best–fit critical point parameters E_c and Γ are listed in 5th and 7th column in Table 1 and presented in Figure 3a for comparison with results of this work. The alloy compositions of the compounds, taken from Ref. [1], are also presented in Table 1.

SE measurements were performed in the photon energies range of 1.5–5 eV with 0.01 eV increment at the room temperature for 70° angle of incidence. The recorded real parts of DF's spectra ε_1 of GaAs$_{1-x}$P$_x$ alloys (A1–A5) containing different P content are shown in Figure 2a. The measured imaginary ε_2 and real parts ε_1 of the DF of sample A2 are represented in Figure 2b as an example. More explanations of these spectra can be seen in Ref. [1, 5]. As clearly seen in Figure 2a, the peaks corresponding to the absorption edge in the real part of the DFs are shifted to higher energies with increasing P content in the alloys. The shifting for the fundamental band E_0 is denoted by arrows in Figure 2a. It is well known that the intensity of the E_2 transition energy is reduced due to the oxide layer on the surface. The surfaces of the samples
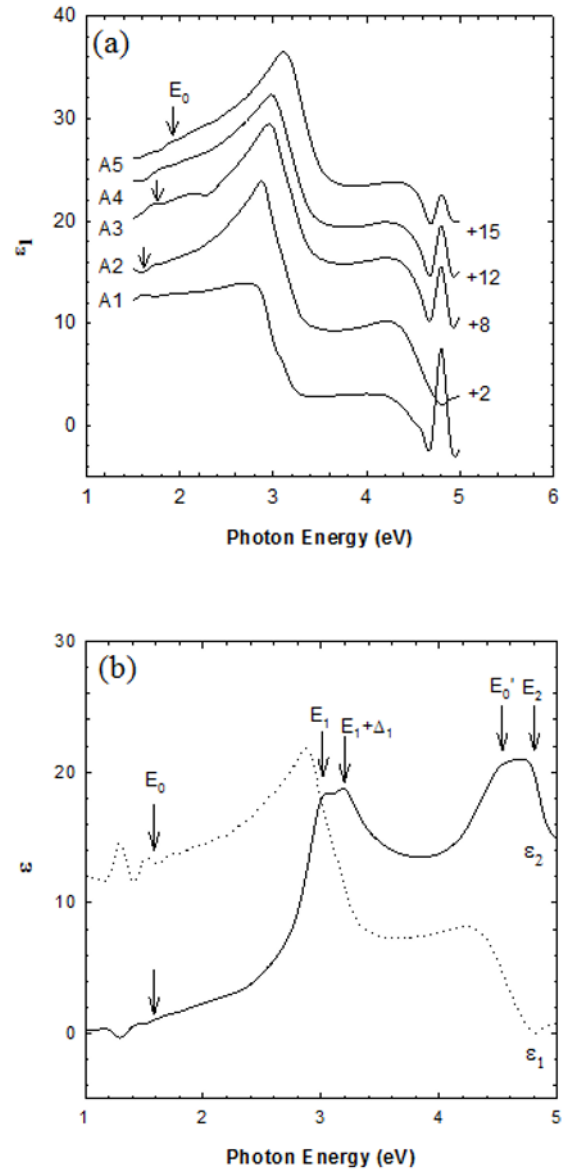

Figure 2. (a) Measured real parts of the dielectric functions of GaAs$_{1-x}$P$_x$ alloys in various alloy compositions, (b) imaginary (dot line) and real parts (solid line) of the dielectric function of Sample A2 [1].

were not chemically etched, since the etching of the surface to remove the oxide overlayer can cause roughness of surface. However, the E_2 transition energy was observed clearly and was well resolved as seen Figure 2. In the imaginary part of the DF ε_2 spectra, four main peaks were observed as seen in solid line in Figure 2b, which correspond to the CP energies of the interband–transition

Cristina-Mihaela Băleanu, Raoul R. Nigmatullin, Saime Sebnem Cetin,
Dumitru Băleanu, Suleyman Ozcelik

edges: $E_0, E_1, E_1 + \Delta_1, E_0'$, and E_2 respectively. The fundamental absorption edge (band gap) E_0 is located at the Γ–point in Brillouin zone. E_1 and $E_1 + \Delta_1$ transitions take place at the Λ–line in Brillouin zone. The Δ_1 is correspondent to the spin–orbit splitting in band at Λ–line. E_0' and E_2 is correspondent to the transition energy near Γ–

point and X–point in the Brillouin zone, respectively. The CP energies of samples may be estimated from experimental ε_2 spectra. As these data are not correspondent to accurate CP energies, several analyzing models had been developed in order to obtain accurate CPs from pure ellipsometric data [28].

Table 1. The critical point (CP) energies, line broadening factors Γ, excitonic phase angle Φ and amplitudes A of the DFs obtained ECs method for GaAs$_{1-x}$P$_x$/GaAs structures. Also, the CP energies and line broadening parameters of the alloys obtained by using line shape analysis (LSA) method including evaluation of the second derivative of the DF are presented to compare with obtained ECs method.

Samples	Alloy composition[a] (%x)		CP Energies (eV)		Parameters			
					Γ (eV)		Φ	A
			ECs	LSA[a]	ECs	LSA[a]		
A1	7	E_0	1.5217	1.510	0.0391	0.0377	-0.7850	1.050
		E_1	2.9361	2.938	0.1077	0.1167	-0.0380	55.365
		$E_1 + \Delta E_1$	3.1838	3.177	0.2829	0.1490	-0.0921	43.670
		E_0'	4.3676	4.370	0.0072	–	1.1374	0.200
		E_2	4.7254	4.740	0.3969	–	-0.0954	106.388
A2	15	E_0	1.6267	1.620	0.0410	0.0510	-1.3960	0.530
		E_1	2.9950	2.969	0.1255	0.1252	-0.0431	144.996
		$E_1 + \Delta E_1$	3.2447	3.178	0.3008	0.1579	-0.0956	136.919
		E_0'	4.3994	4.400	0.0203	–	1.5708	0.058
		E_2	4.7470	4.750	0.5088	–	-0.1187	242.228
A3	23	E_0	1.7162	1.710	0.0498	0.0536	1.5708	0.417
		E_1	3.0343	3.051	0.1335	0.1530	-0.0452	146.595
		$E_1 + \Delta E_1$	3.2870	3.305	0.3538	0.1874	-0.1109	139.860
		E_2	4.7902	4.440	0.0347	–	-0.4907	0.828
		E_0'	4.4280	4.790	0.5952	–	-0.1376	261.611
A4	32	E_0	1.7881	1.780	0.0102	0.0611	-1.0291	0.168
		E_1	3.0857	3.061	0.1502	0.1710	-0.0500	102.948
		$E_1 + \Delta E_1$	3.3420	3.350	0.3782	0.1913	-0.1474	116.715
		E_0'	4.4616	4.470	0.0251	–	-0.3934	0.905
		E_2	4.7906	4.790	0.2691	–	-0.0620	215.254
A5	39	E_0	1.9142	1.910	0.0246	0.0714	1.5708	0.104
		E_1	3.1100	3.190	0.1633	0.1860	-0.0540	98.814
		$E_1 + \Delta E_1$	3.3915	3.367	0.3815	0.1991	-0.1160	116.925
		E_0'	4.4874	4.540	0.0499	–	-0.4010	s 1.200
		E_2	4.8279	4.820	0.2051	–	-0.0470	221.573

[a]Taken from Ref. [1]

Using the measured real part of the DF data which are given Figure 2a, values of the critical point energy E_c, the broadening factor Γ and the excitonic phase angle Φ, and also amplitude A of the DF against the concentration x in the alloys, can be calculated with the help of expressions (5, 6) and (10, 11). The calculated results using ECs method are presented in Table 1 and also shown on Figure 3b. As seen in Table 1, the obtained values of CPs energies using ECs method were in good agreement with the ones calculated by line shape analysis (LSA) method including the evaluations of the second derivative of the

DF of the GaAsP heterostructures. The broadenings of the CP energies, calculated with these two methods, increases with increasing phosphorous composition as seen in the Table 1 and in Figure 4. The increase in broadening can be explained by alloy scattering, statistical fluctuations, and large–scale compositional variations [1, 30]. The values of the broadening factor in case of the ECs method are bigger than obtained by LSA method. This may be explained with capability of noise reduction of the ECs method. Also, the line broadening of the E$_0'$ and E_2 transitions could be calculated by ECs method although there

were difficulties to obtain them with LSA method for these samples.

In comparing Figure 3a and 3b, it can be seen that the change of the CP energies, obtained using LSA method (including second derivative) in our previous work [1] and the ECs method, versus P composition in the samples, have a similar trend. Also, as seen in Figure 3b, the bow-

ing parameter (b) for the fundamental transition energy E_0 has been found as 0.218 eV. The bowing of the band gap energy is due to disordered phosphorous content in the ternary alloy. Obtained bowing parameter using ECs methods is very close to the value of the obtained second derivative method [1] as seen in Figure 3a, and also to the reported theoretical and experimental values [29].
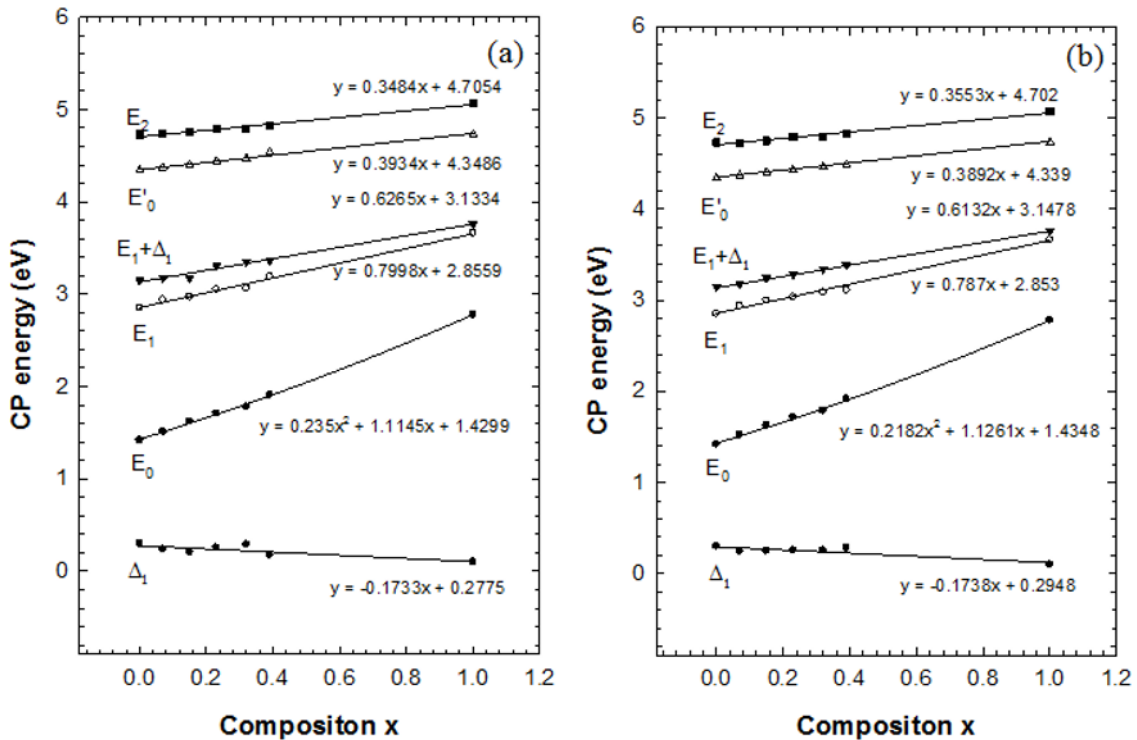

Figure 3. The calculated critical point energies $E_0, E_1, E_1 + \Delta_1, E_0'$ and E_2 transition edges of GaAs$_{1-x}$P$_x$/GaAs structures using (a) line-shape analysis method [1] (b) Eigen-coordinates method. The dots show the calculated values, and the solid lines correspond to the fits. As seen figures (a) and (b), obtained CP energy values and the bowing of the band gap energy versus P content in the alloys gained by using these two computational methods are very close. Also, the spin-orbit splitting energy is reduced by increasing P composition. (Critical point energies, $E_0, E_1, E_1 + \Delta_1, E_0'$ and E_2 values of GaAs and GaP were taken by Ref. [2].)

5. Basic conclusions

We presented a new method that can be used for calculation of the critical points energies and the bowing parameter of the band gap energy due to disordered phosphorous content of the GaAs$_{1-x}$P$_x$/GaAs (100) ternary alloys, which are grown by using MBE. Here, we also want to stress the importance of applications of the original ECs method for calculation of the critical points. The tra-

ditional method [1] related to calculation of the critical points is based on the calculation of the second derivatives from Equation (1) and subsequent fitting realized with the necessary polynomials depending on the order n. But this method is not free from uncontrollable errors related to calculation of the second derivative, subsequent smoothing and fitting of the noisy data that also contain the uncontrollable errors. The new method can be considered as alternative to the conventional method and has

Cristina-Mihaela Băleanu, Raoul R. Nigmatullin, Saime Sebnem Cetin,
Dumitru Băleanu, Suleyman Ozcelik

the following advantages:

1. It does not use any derivatives and the derivative operation in some cases is replaced by integration (that can be considered as the natural smoothing procedure).

2. The basic linear relationship that is mathematically equivalent to initial functions in Equation (1) helps

to find the global fitting minima including the values of the critical points. This important feature undoubtedly increases the level of significance in calculation of the critical points.
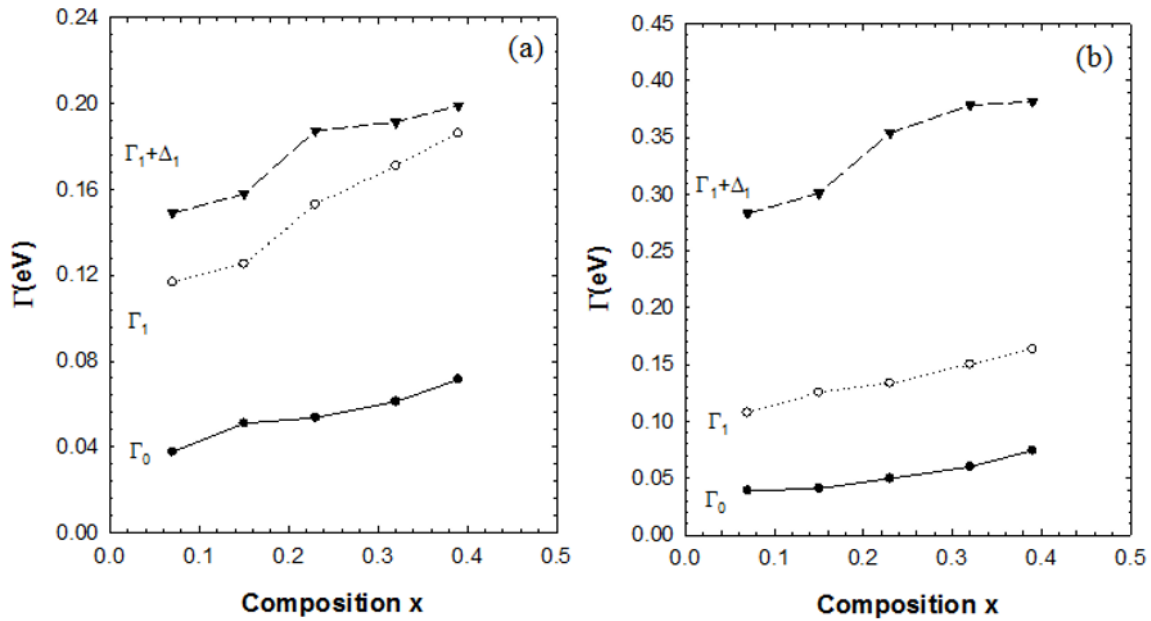
Figure 4. The broadening factors Γ corresponding to E_0, E_1, and $E_1 + \Delta_1$ using (a) line-shape analysis [1] (b) Eigen-coordinates method. The broadening of the CPs is increased with increasing the P content.

Appendix A: Mathematical appendix

The application of the ECs method to our problem is explained in detail below.
We present two cases, namely when $n = 0$ and $n \neq 0$.

Case 1

The starting point is the expression of

$$\varepsilon(E) = C - Ae^{i\Phi}\ln(E - E_c + i\Gamma)n = 0. \qquad (A1)$$

The photon energy E can be modified experimentally. The fitting parameters are C, A, Φ, E_c, Γ.

Our aim is to linearize the expression of (A1), where $\varepsilon \equiv y + iz$, where $y = \Re\varepsilon$ and $z = \Im\varepsilon$.
By using $e^{i\Phi} = \cos\Phi + i\sin\Phi$ we obtain

$$\ln(E - E_c + i\Gamma) = \ln r + i\theta, \qquad (A2)$$

where

$$r = \sqrt{(E - E_c)^2 + \Gamma^2}$$

and

$$\theta = \arctan\frac{\Gamma}{E - E_c}.$$

As a result we obtain

$$
\begin{aligned}
\varepsilon(E) &= C - Ae^{i\Phi}\ln(E - E_c + i\Gamma) \\
&= C - A(\cos\Phi + i\sin\Phi)(\ln r + i\theta),
\end{aligned} \tag{A3}
$$

or

$$
\begin{aligned}
\varepsilon(E) &= C - A(\ln r \cos\Phi - \theta\sin\Phi) \\
&\quad - Ai(\ln r \sin\Phi + \theta\cos\Phi).
\end{aligned} \tag{A4}
$$

Finally, we identify the real and the imaginary part of $\varepsilon(E)$ as

$$
\Re(\varepsilon(E)) = y = C - A(\ln r \cos\Phi - \theta\sin\Phi), \tag{A5}
$$

$$
\Im(\varepsilon(E)) = z = -A(\ln r \sin\Phi + \theta\cos\Phi), \tag{A6}
$$

$$
C - y = A\ln r \cos\Phi - A\theta\sin\Phi, \tag{A7}
$$

$$
z = -A(\ln r \sin\Phi + \theta\cos\Phi). \tag{A8}
$$

By taking the derivative with respect with to E we obtain

$$
\begin{aligned}
(\ln r)' &= \frac{\frac{dr}{dE}}{r} = \frac{E - E_c}{(E - E_c)^2 + \Gamma^2}, \\
\frac{d\theta}{dE} &= \frac{-\Gamma}{(E - E_c)^2 + \Gamma^2},
\end{aligned} \tag{A9}
$$

$$
y' = -A\cos\Phi\,(\ln r)' + A\sin\Phi\frac{d\theta}{dE}, \tag{A10}
$$

$$
z' = -A\sin\Phi\,(\ln r)' - A\cos\Phi\frac{d\theta}{dE}. \tag{A11}
$$

Finally we obtain:

$$
\begin{aligned}
y' = &-A\cos\Phi\frac{E - E_c}{(E - E_c)^2 + \Gamma^2} \\
&+ A\sin\Phi\frac{-\Gamma}{(E - E_c)^2 + \Gamma^2},
\end{aligned} \tag{A12}
$$

$$
\begin{aligned}
z' = &-A\sin\Phi\frac{E - E_c}{(E - E_c)^2 + \Gamma^2} \\
&- A\cos\Phi\frac{-\Gamma}{(E - E_c)^2 + \Gamma^2}.
\end{aligned} \tag{A13}
$$

We can write that

$$
\begin{aligned}
\ln r &= \frac{1}{r^2}\begin{vmatrix} C - y & -A\sin\Phi \\ -z & A\cos\Phi \end{vmatrix} \\
&= \frac{1}{A^2}[(C - y)A\cos\Phi - Az\sin\Phi] \\
&= \frac{(C - y)\cos\Phi}{A} - \frac{z\sin\Phi}{A}.
\end{aligned} \tag{A14}
$$

Let us make the following notations $u = A\ln r$ and $v = A\theta$. As a result we obtain

$$
\begin{aligned}
C - y &= \cos\Phi u - \sin\Phi v, \\
-z &= \sin\Phi u + \cos\Phi v.
\end{aligned} \tag{A15}
$$

By using the Cramer's method we obtain the following solutions

$$
u = \begin{vmatrix} C - y & -\sin\Phi \\ -z & \cos\Phi \end{vmatrix} = (C - y)\cos\Phi - z\sin\Phi, \tag{A16}
$$

$$
v = \begin{vmatrix} \cos\Phi & C - y \\ -\sin\Phi & -z \end{vmatrix} = -(C - y)\sin\Phi - z\cos\Phi. \tag{A17}
$$

At this stage we take the derivatives of u and v with respect to E and we obtain

$$
u' = -\cos\Phi y' - \sin\Phi z' = A\frac{(E - E_c)}{(E - E_c)^2 + \Gamma^2}, \tag{A18}
$$

$$
v' = \sin\Phi y' - \cos\Phi z' = -A\frac{\Gamma}{(E - E_c)^2 + \Gamma^2}. \tag{A19}
$$

From (A18) and (A19) we obtain

$$
\begin{aligned}
y\cos\Phi y' + y\sin\Phi z' = &(E - E_c)\sin\Phi y' \\
&- (E - E_c)\cos\Phi z'
\end{aligned} \tag{A20}
$$

or

$$
\frac{(E - E_c)}{\Gamma} = \frac{\cos\Phi y' + \sin\Phi z'}{\sin\Phi y' - \cos\Phi z'}. \tag{A21}
$$

As a result we get

$$
\begin{aligned}
Ey' = &E_c.y' - E_c.\cot\Phi.z' + E.\cot\Phi.z' \\
&+ \Gamma\cot\Phi.y' + y.z'.
\end{aligned} \tag{A22}
$$

Taking into account that

$$
y'\left[(E - E_c)^2 + \Gamma^2\right] = -A\cos\Phi\,(E - E_c) - \Gamma A\sin\Phi, \tag{A23}
$$

$$
\begin{aligned}
y'E^2 + y'E_c^2 + y'\Gamma^2 - 2EE_c y' = &-A\cos\Phi E + A\cos\Phi E_c \\
&- \Gamma A\sin\Phi
\end{aligned} \tag{A24}
$$

we conclude that

$$
\begin{aligned}
y'E^2 = &2EE_c y' - y'\left(E_c^2 + \Gamma^2\right) - A\cos\Phi E \\
&+ A(\cos\Phi E_c - \Gamma\sin\Phi).
\end{aligned} \tag{A25}
$$

By integration followed by a separation of terms which do not contain to the left hand side we obtain

$$T_0 = \int y'E^2 dE = yE^2 - 2\int_{y_0}^{y} yE dE$$

$$= E^2 y - E_0^2 y_0 - 2\int yE dE,$$

(A26)

$$T_1 = \int 2E_c E y' dE = 2E_c \int_{y_0}^{y} y'E dE$$

$$= 2E_c \left(Ey - \int y dE \right)$$

$$= 2E_c E - 2E_c \int y dE - 2E_c E_0 y_0,$$

(A27)

$$T_2 = \int \left(E_c^2 + \Gamma^2 \right) y' dE = \left(E_c^2 + \Gamma^2 \right) \int y' dE$$

$$= \left(E_c^2 + \Gamma^2 \right) y - \left(E_c^2 + \Gamma^2 \right) y_0,$$

(A28)

$$T_3 = \int -A\cos\Phi E dE = -A\cos\Phi \int E dE$$

$$= -A\cos\Phi \frac{E^2}{2} + A\cos\Phi \frac{E_0^2}{2},$$

(A29)

$$T_4 = \int (A\cos\Phi E_c) dE = A\cos\Phi E_c \int dE$$

$$= A\cos\Phi E_c E - A\cos\Phi E_c E_0,$$

(A30)

$$T_5 = \int -A\sin\Phi \Gamma dE = -A\sin\Phi \Gamma E + A\sin\Phi \Gamma E_0.$$ (A31)

By regrouping the terms we obtain

$$yE^2 - 2\int yE dE - E_0^2 y_0 = 2E_c E - 2E_c \int y dE$$
$$-2E_c E_0 y_0 - \left(E_c^2 + \Gamma^2 \right) y + \left(E_c^2 + \Gamma^2 \right) y_0$$
$$-A\cos\Phi \frac{E^2}{2} + A\cos\Phi \frac{E_0^2}{2} + A\cos\Phi E_c E$$
$$-A\cos\Phi E_c E_0 - A\sin\Phi \Gamma E + A\sin\Phi \Gamma E_0.$$

(A32)

All terms containing E_0 and y_0 are constants and we include them to $\langle \ldots \rangle$ which denotes the average of the error subtraction. Therefore, we obtain

$$Y = yE^2 - 2\int yE dE - \langle \ldots \rangle.$$ (A33)

Taking into account that Y is of the form

$$Y = C_1 X_1 + C_2 X_2 + C_3 X_3 + C_4 X_4.$$ (A34)

By identification we obtain the constants C_i and X_i as given below

$$X_1 = yE - \int y dE - \langle \ldots \rangle, \quad C_1 = 2E_c,$$

$$X_2 = y - \langle \ldots \rangle, \quad\quad\quad C_2 = -\left(E_c^2 + \Gamma^2 \right),$$

$$X_3 = E^2 - \langle \ldots \rangle, \quad\quad\quad C_3 = -\frac{A\cos\Phi}{2},$$

$$X_4 = E - \langle \ldots \rangle, \quad\quad\quad C_4 = A\cos\Phi E_c - \Gamma A\sin\Phi.$$

(A35)

We notice that E_c is very important in finding the critical point. We can solve the system of equations with respect with the fitting parameters and we obtain the following results

$$E_c = \frac{C_1}{2}, \quad \Gamma = \pm\sqrt{-C_2 - \frac{C_1^2}{4}}.$$ (A36)

We notice that

$$A\cos\Phi = -2C_3,$$
$$A\Gamma\sin\Phi = -C_1 C_3 - C_4$$

and

$$A\sin\Phi = -\frac{(C_1 C_3 + C_4)}{\sqrt{-C_2 - \frac{C_1^2}{4}}}.$$

Case 2

By analogy one can obtain the next BLR.
In this case the expression to start with is $\varepsilon(E) = C + Ae^{i\Phi}\ln(E - E_c + i\Gamma)^n$, $n \neq 0$.
The fitting parameters are the same as before. As a result we obtain

$$(E - E_c + i\Gamma)^n = r^n e^{ni\theta},$$ (A37)

where

$$r = \sqrt{(E - E_c)^2 + \Gamma^2}$$

and

$$\theta = \arctan\frac{\Gamma}{E - E_c}.$$

By inspection we observe that

$$(E - E_c + i\Gamma)^n = (\cos\Phi + i\sin\Phi) r^n (\cos n\Phi + i\sin n\Phi)$$
$$= r^n \left[(\cos\Phi\cos n\theta - \sin\Phi\sin n\theta) \right.$$
$$\left. + i(\sin\Phi\cos n\theta + \cos\Phi\sin n\theta) \right]$$
$$= r^n \left[\cos(\Phi + n\theta + \pi) \right.$$
$$\left. + i\sin(\Phi + n\theta + \pi) \right]$$

(A38)

or can write it as

$$(E - E_c + i\Gamma)^n = r^n \left[\cos\left(\Phi' + n\theta\right) + iA\sin\left(\Phi' + n\theta\right) \right], \tag{A39}$$

under $\Phi = \Phi' + \pi$.
We recall that

$$\varepsilon(E) - C = Ar^n \left[\cos\left(\Phi' + n\theta\right) \right] + iA\sin\left[\left(\Phi' + n\theta\right) \right]$$
$$\equiv y + iz \tag{A40}$$

or

$$y - C = Ar^n \cos\left(\Phi' + n\theta\right), \quad z = Ar^n \sin\left(\Phi' + n\theta\right). \tag{A41}$$

Taking the logarithm we obtain

$$\ln(y - C) = \ln A + n\ln r + \ln(\cos(\Phi' + n\theta)). \tag{A42}$$

By using a similar procedure as before, we take the derivative with respect to energy E and we obtain

$$(\ln r)' = \frac{\frac{dr}{dE}}{r} = \frac{E - E_c}{(E - E_c)^2 + \Gamma^2}$$

or

$$\frac{\frac{dr}{dE}}{r} = \frac{(E - E_c)}{(E - E_c)^2 + \Gamma^2}, \tag{A43}$$

$$\frac{d\theta}{dE} = \frac{-\Gamma}{(E - E_c)^2 + \Gamma^2}. \tag{A44}$$

Therefore we find out that

$$y'\left[(E - E_c)^2 + \Gamma^2\right] = n(E - E_c)(y - C) + \Gamma zn. \tag{A45}$$

By making use of the separation of terms we obtain

$$E^2 y' = 2y' E E_c - \left(E_c^2 + \Gamma^2\right) y' + nyE - nCE$$
$$- nyE_c + \Gamma zn + nE_c C. \tag{A46}$$

Following similar technique as in Case 1 and taking into account that Y is given below

$$Y = C_1 X_1 + C_2 X_2 + C_3 X_3 + C_4 X_4 + C_5 X_5. \tag{A47}$$

By identification we obtain

$$Y = yE^2 - (n + 2)\int EydE - \langle\ldots\rangle, \tag{A48}$$

$$X_1 = 2yE - (n + 2)\int ydE - \langle\ldots\rangle, \tag{A49}$$

$$X_2 = y - \langle\ldots\rangle, \tag{A50}$$

$$X_3 = \frac{nE^2}{2} - \langle\ldots\rangle, \tag{A51}$$

$$X_4 = n\int zdE, \tag{A52}$$

$$X_5 = nE - \langle\ldots\rangle. \tag{A53}$$

The constants are given by

$$\begin{aligned} C_1 &= E_c, \\ C_2 &= -\left(E_c^2 + \Gamma^2\right), \\ C_3 &= C, \\ C_4 &= \Gamma, \\ C_5 &= CE_c. \end{aligned} \tag{A54}$$

We observe that

$$C_1.C_3 = C_5 \quad \text{and} \quad C_2 = -\left(C_1^2 + C_4^2\right). \tag{A55}$$

Finally we conclude that

$$\Gamma = \left[-\left(E_c + C_2^2\right) \right]^{\frac{1}{2}}, \tag{A56}$$

and

$$\Phi = \arctan\left(\frac{-2C_2\Gamma}{C_3 + 2C_2 AE_c} \right). \tag{A57}$$

Acknowledgments

References

[1] S.S. Cetin, T.S. Mammadov, S. Ozcelik, Optoelectron. Adv. Mat. 3, 910 (2009)

[2] K.J. Kim, M.H. Lee, J.H. Bahng, K. Shim, B.D. Choe, J. Appl. Phys. 84, 3696 (1998)

[3] N.B. Sedrine, J. Rihani, J.L. Stehle, J.C. Harmand, R. Chtourou, Mater. Sci. Eng. C 28, 640 (2008)

[4] T.H. Ghong, T.J. Kim, Y.W. Jung, Y.D. Kim, D.E. Aspnes, J. Appl. Phys. 103, 073502 (2008)

[5] S.S. Cetin et al., Surf. Interface Anal. 42, 1252 (2010)

[6] A.B. Djurisic, Y. Chan, E. Helbert, Mater. Sci. Eng. R38, 237 (2002)

[7] J.J. Yoon et al., Appl. Surf. Sci. 256, 1031 (2009)

[8] R.R. Nigmatullin, Appl. Magn. Reson. 14, 601 (1998)

[9] R.R. Nigmatullin, Physica A 285, 547 (2000)

[10] M.M. Abdul-Gader Jafar, R.R. Nigmatullin, Thin Solid Films 396, 280 (2001)

[11] R.R. Nigmatullin, M.M. Abdul-Gader Jafar, N. Shinyashiki, S. Sudo, S. Yagihara, J. Non-Cryst. Solids 305, 96 (2002)

[12] R.R. Nigmatullin, S.I. Osokin, G. Smith, J. Phys.-Condens. Mat. 15, 3481 (2003)

[13] R.R. Nigmatullin, S.I. Osokin, G. Smith, J. Phys. D Appl. Phys. 36, 2281 (2003)

[14] R.R. Nigmatullin, Physica B 358, 201 (2005)

[15] R.R. Nigmatullin, A.L. Mehaute, J. Non-Cryst. Solids 351, 2888 (2005)

[16] R.R. Nigmatullin, Physica A 363, 282 (2006)

[17] R.R. Nigmatullin, S.O. Nelson, Signal Process. 86, 2744 (2006)

[18] R.R. Nigmatullin, S.O. Nelson, IEEE T. Dielect. El. In. 13, 1325 (2006)

[19] R.R. Nigmatullin et al., Physica B 388, 418 (2007)

[20] R.R. Nigmatullin, A.A. Arbuzov, F. Salehli, A. Gis, H. Catalgil-Giz, J. Non-Cryst. Solids 353, 4143 (2007)

[21] R.R. Nigmatullin, Physica B 404, 255 (2009)

[22] R.R. Nigmatullin, Commun. Nonlinear Sci. 15, 637 (2010)

[23] M. Al-Hasan, R.R. Nigmatullin, Renew. Energ. 28, 93 (2003)

[24] R.R. Nigmatullin, G. Smith, Physica A 320, 291 (2003)

[25] R.R. Nigmatullin, Phys. Wave Phenom. 16, 119 (2008)

[26] V.V. Afanasiev, R.R. Nigmatullin, Y.E. Polsky, Tech. Phys. Lett.+ 30, 675 (2004)

[27] H. Fujiwara, Spectroscopic Ellipsometry Principles and Applications (John Wiley & Sons, New York, 2007)

[28] S. Adachi, Phys. Rev. B 38, 12345 (1988)

[29] M. Bugajski, A.M. Kontkiewicz, H. Mariette, Phys. Rev. B 28, 7105 (1983)

[30] C.S. Cook et al., Thin Solid Films 455, 217 (2004)